Progress In Electromagnetics Research Letters, Vol. 78, 39–43, 2018

Comment on "Frequency Tunable Low-Cost Microwave Absorber for EMI/EMC Application" by Gobinda Sen and Santanu Das in *Progress In Electromagnetics Research Letters*, Vol. 74, 47–52, 2018

Hao Zhang[1], Yu Ma[1], Hai Feng Zhang[1, 2, 3, 4, *], Jing Yang[1], and Jia-Xuan Liu[1]

Abstract—In a recently published report, Sen and Das [5] proposed a frequency tunable low-cost microwave absorber to obtain tunable absorption spectra. In this paper, we justify that the proposed device is not an absorber. It is observed that the total absorption rates merely reach 2% and 14.85% for the air gaps of 3.5 mm and 7.5 mm, respectively, when the co- and cross-polarization reflections are taken into account in the reported device. Obviously, The original authors erroneously consider a polarization converter as an absorber, and the obvious errors can be found in their paper.

1. INTRODUCTION

In recent years, metamaterial absorbers, as a novel research field of electromagnetic metamaterials, have attracted extensive research interest for the application of physics and material science. Tunable absorber [1, 2] is drawing great attention due to the flexible adjustable frequency region. Nowadays, many methods have been proposed to achieve frequency reconfigurability. A dual-band tunable perfect metamaterial absorber was presented by Yao et al. [3], where tunable resonance frequency can be obtained by regulating the Fermi level of graphene. Li et al. [4] utilized an active frequency selective surface to devise a tunable low-frequency and broadband radar absorber, which shows that the resonance frequencies shift with changing the capacitance of the impedance layer. In a recent paper entitled "Frequency Tunable Low-Cost Microwave Absorber for EMI/EMC Application", a frequency tunable low-cost microwave absorber was devised by Sen and Das [5], as shown in Fig. 1. The original authors demonstrated that the absorption can be tuned through changing the air gap (G) between the substrates. The absorption spectrum for the gap of 3.5 mm displays a signal distinct absorption peak situated at 12.46 GHz. If the thickness of air gap is 7.5 mm, the designed absorber shows that two strong absorption peaks are located at 11.22 GHz and 15.54 GHz, respectively. However, some issues of mixed polarization may be neglected in the design of such an absorber. Therefore, some explanations are illustrated in the comment.

The transmission is zero on account of the shielding by the metal plate. Therefore, the absorption efficiency of the proposed absorber can be characterized as $A(\omega) = 1 - R(\omega) = 1 - |S_{11}(\omega)|^2$, where reflection parameter ($S_{11}(\omega)$) can be expressed as $|S_{11}(\omega)|^2 = |S_{TETE}(\omega)|^2 + |S_{TMTE}(\omega)|^2$. It is noted that $|S_{TETE}(\omega)|^2$ and $|S_{TMTE}(\omega)|^2$ can be calculated by co-polarization and cross-polarization, respectively. It can be found that the values of the parameters in Table 1 apparently do not correspond

Received 26 May 2018, Accepted 23 July 2018, Scheduled 24 August 2018

* Corresponding author: Hai Feng Zhang (hanlor@163.com).

[1] College of Electronic and Optical Engineering & College of Microelectronics, Nanjing University of Posts and Telecommunications, Nanjing 210023, China. [2] National Electronic Science and Technology Experimental Teaching Demonstrating Center, Nanjing University of Posts and Telecommunications, Nanjing 210023, China. [3] National Information and Electronic Technology Virtual Simulation Experiment Teaching Center, Nanjing University of Posts and Telecommunications, Nanjing 210023, China. [4] College of Electronic and Information Engineering, Nanjing University of Aeronautics and Astronautics, Nanjing 210016, China.

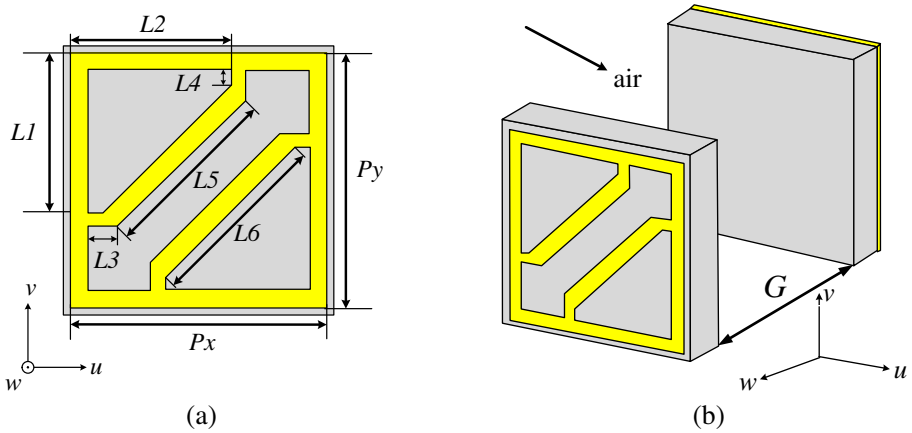

Figure 1. (a) The unit cell dimensions of proposed frequency selective surface. (b) Schematic of the proposed absorber.

Table 1. The parameters of the proposed absorber (in mm).

Px	Py	$L1$	$L2$	$L3$	$L4$	$L5$	$L6$
6.3	6.3	3.6	3.6	1	0.4	2.83	3.54

to the dimensions of the schematic in [5]. Then, the reflected spectra of the different values of parameter $L2$ ($L1 = L2$) for the air gap of 7.5 mm are simulated according to the size ratio of the schematic in [5]. The parameters as mentioned in [5] are not corrected obviously. The corresponding spectra are plotted in Figs. 2(a)–(c), which show that the cross-polarized reflection is very high regardless of the value of $L2$. Compared to the spectrum ($G = 7.5$ mm) in [5], the spectrum at $L2 = 3.6$ mm is consistent basically. The corresponding parameters of the unit cell are shown in Table 1. As shown in Fig. 2(d), there is only a absorption peak located at 13.68 GHz with absorption rate of 14.85% when the cross-polarization is considered. At the same time, the simulated reflection spectra and total absorptivity for the air gap of 3.5 mm are depicted in Fig. 3. It can be seen from Fig. 3(b) that the absorption rate is only 2%. Moreover, the absorption spectra for the air gap of 3.5 mm at various incident angles are displayed in Fig. 4. Comparing Fig. 4 with Fig. 8 in [5], the cross-polarization reflection is not taken into account distinctly when the absorption is calculated.

The polarization conversion radio (PCR) is defined by $PCR = |S_{TMTE}|^2 \Big/ \left(|S_{TMTE}|^2 + |S_{TETE}|^2\right)$, which can be used to measure the efficiency of polarization conversion. The polarization conversion radio spectrum ($G = 3.5$ mm) is given in Fig. 5(a), which shows that PCR is higher than 99.7% at 12.34 GHz. Furthermore, when the air gap is 7.5 mm it can be observed from Fig. 5(b) that there are three strong peaks at 11.05 GHz, 13.69 GHz and 15.67 GHz with the PCR of 99.78%, 95.16% and 99.9%, respectively. Evidently, the designed device is a polarization converter [6, 7] with good performance.

To better interpret the physical mechanism of polarization conversion, the calculated distributions of surface current for the air gap of 3.5 mm are plotted in Fig. 6. As shown in Fig. 6, the induced electric field $\mathbf{E}$ along the direction of induced currents (see the purple arrow in Figs. 6(a) and 6(b)) can be decomposed into two components, namely horizontal component $\mathbf{E}_x$ and perpendicular component $\mathbf{E}_y$. The electric field components of the top and bottom surfaces in the x direction are anti-parallel, indicating the magnetic coupling. The induced magnetic field $\mathbf{H}$ has horizontal and perpendicular components ($\mathbf{H}_x$ and $\mathbf{H}_y$). On the basis of the definition of transverse electric and transverse magnetic polarization, the coactions of $\mathbf{E}_y$ and $\mathbf{H}_x$ produce the reflection of transverse electric wave, and the reflection of transverse magnetic wave is formed owing to the coupling between $\mathbf{E}_x$ and $\mathbf{H}_y$. As described above, the reflection of incident electromagnetic wave is composed of two parts (transverse electric wave and transverse magnetic wave). The absorption and polarization conversion are caused by transverse electric wave and transverse magnetic wave, respectively.

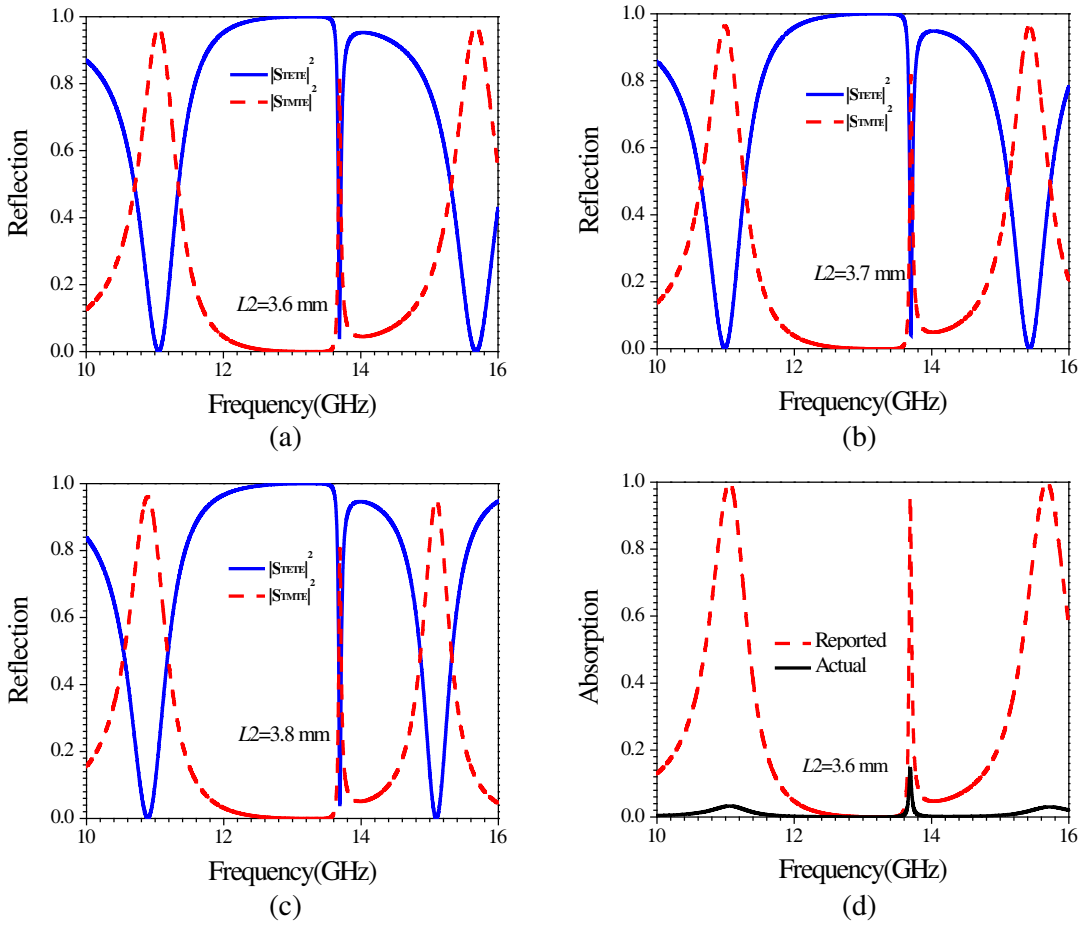

Figure 2. (a)–(c) the simulated spectra of $|S_{TETE}(\omega)|^2$ and $|S_{TMTE}(\omega)|^2$ for the different values of parameter $L2$, (d) the simulated absorption spectrum in Ref. [5] and the actual absorption spectrum for the air gap of 7.5 mm.

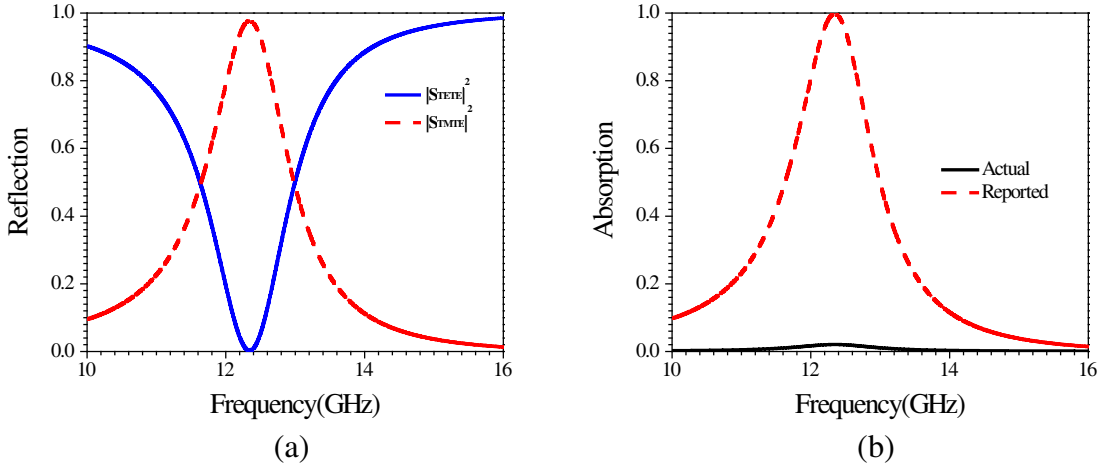

Figure 3. (a) The simulated spectra of $|S_{TETE}(\omega)|^2$ and $|S_{TMTE}(\omega)|^2$ ($G = 3.5$ mm), (b) the simulated absorption spectrum in Ref. [5] and the actual absorption spectrum for the air gap of 3.5 mm.

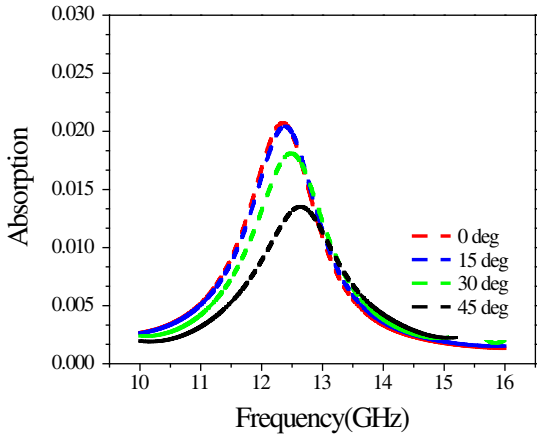

Figure 4. The total absorption spectra at various incident angles ($G = 3.5\,\text{mm}$).

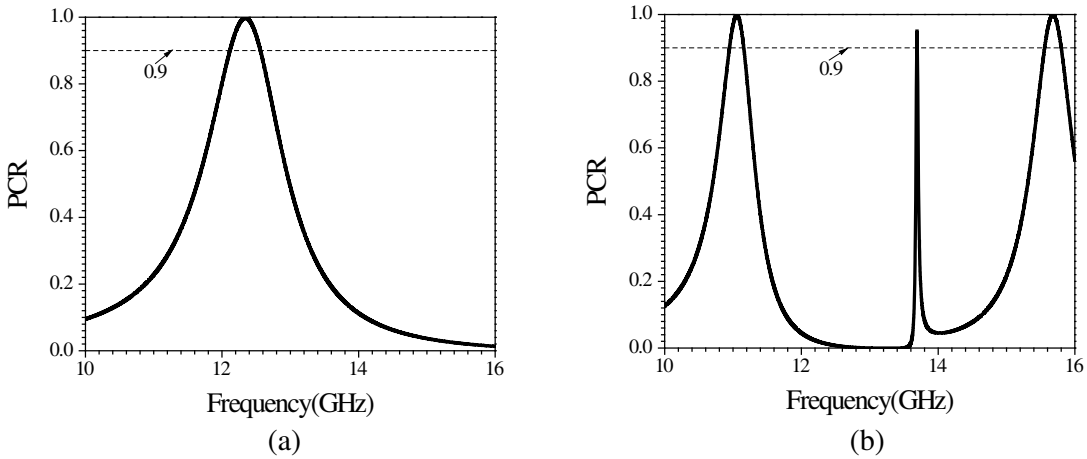

Figure 5. The simulated PCR for (a) $G = 3.5\,\text{mm}$ and (b) $G = 7.5\,\text{mm}$.

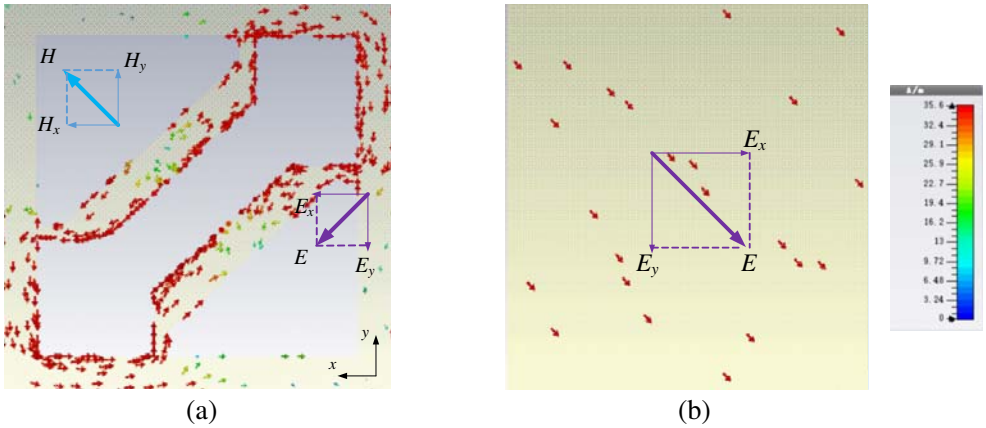

Figure 6. The distributions of surface current at 12.34 GHz, (a) on the top plane, and (b) on the bottom plane.

2. CONCLUSIONS

In conclusion, the designed absorber in [5] has merely perfect absorbing performance due to polarization conversion. The designed structure is symmetrical along the diagonal. The polarization conversion may occur owing to such a structure. Thus, the cross-polarization should be taken into account to determine whether PCR is relatively high when an absorber is proposed.

REFERENCES

1. Zhai, H. Q., C. H. Zhan, L. Liu, and C. H. Liang, "A new tunable dual-band metamaterial absorber with wide-angle TE and TM polarization stability," *Journal of Electromagnetic Waves and Applications*, Vol. 29, No. 6, 774–785, 2015.
2. Xiong, H., Y. B. Wu, J. Dong, M. C. Tang, Y. N. Jiang, and X. P. Zeng, "Ultra-thin and broadband tunable metamaterial graphene absorber," *Opt. Express*, Vol. 26, No. 2, 1681–1688, 2018.
3. Yao, G., F. R. Ling, J. Yue, C. Y. Luo, J. Ji, and J. Q. Yao, "Dual-band tunable perfect metamaterial absorber in the THz range," *Opt. Express*, Vol. 24, No. 2, 1518–1527, 2016.
4. Li, J. L., J. J. Jiang, Y. He, W. H. Xu, M. Chen, L. Miao, and S. W. Bie, "Design of a tunable low-frequency and broadband radar absorber based on active frequency selective surface," *IEEE Antennas Wireless Propag. Lett.*, Vol. 15, 774–777, 2016.
5. Sen, G. and S. Das, "Frequency tunable low cost microwave absorber for EMI/EMC application," *Progress In Electromagnetics Research Letters*, Vol. 74, 47–52, 2018.
6. Liu, X. B., J. S. Zhang, W. Li, R. Lu, L. M. Li, Z. Xu, and A. X. Zhang, "Three-band polarization converter based on reflective metasurface," *IEEE Antennas Wireless Propag. Lett.*, Vol. 16, 924–927, 2017.
7. Huang, X. J., D. Yang, and H. L. Yang, "Multiple-band reflective polarization converter using U-shaped metamaterial," *J. Appl. Phys.*, Vol. 115, No. 10, 103505, 2014.